TENSILE PERFORMANCE OF LIME-BASED NATURAL-FIBRE COMPOSITES AS STRENGTHENING SYSTEMS FOR MASONRY

N. Trochoutsou[1]*, M. Di Benedetti[2], K. Pilakoutas[1], M. Guadagnini[1]

[1] Department of Civil and Structural Engineering, University of Sheffield, Sheffield, S1 3JD, UK

[2] Multidisciplinary Engineering Education, University of Sheffield, Sheffield, S1 3JD, UK

*Corresponding author; e-mail: ntrochoutsou1@sheffield.ac.uk

Abstract

Past earthquakes have highlighted the vulnerability of unreinforced masonry structures, especially in developing countries where non-engineered, masonry buildings make up the majority of the existing building stock. The use of natural fibres, which are readily available and abundant in these countries, has recently emerged as a cost-effective and sustainable strengthening solution. Although the performance of short dispersed natural fibres in inorganic binders has been examined in the literature, the behaviour of natural textile-reinforced mortars (NTRM) as externally bonded strengthening systems is still unknown.

This paper presents some preliminary results of a larger experimental programme on the mechanical performance of natural fibre grids embedded in lime-based mortars. Bare flax and jute yarns and textiles were tested in direct tension to characterise their mechanical properties. NTRM specimens reinforced with the same textiles were also tested to examine their tensile behaviour and assess the contribution of the fibres and mortar to their overall performance. Digital image correlation was used to obtain full-field displacement measurements on the NTRM composites to assist with the development of constitutive models.

The effect of different textile architectures and fibre type is discussed in detail and the potential use of NTRM to strengthen deficient masonry structures is assessed and commented upon.

Keywords:

TRM; tensile tests; DIC; masonry

1 INTRODUCTION

Failures and collapses of unreinforced masonry (URM) elements during past earthquake events (Turkey, 1999; Haiti and Chili, 2010; Nepal, 2015; Italy, 2017; Mexico, 2017) highlighted the seismic vulnerability of these structures and resulted in numerous casualties and catastrophic damage to buildings and civil infrastructure. With masonry construction requiring low cost materials and technologies, masonry is one of the most used construction materials in developing countries, which have suffered the most from seismic events.

Strengthening of URM structures using natural fibres arises as a promising solution that could be easily implemented in less favoured economies. Natural fibres are readily available and abundant: 25 million tons of natural fibres are produced globally per annum, 25% of which are produced in India [Dunne 2016]. Moreover, natural fibres are affordable, costing up to three times less than synthetic fibres on the basis of raw material per kg [Dittenber 2012].

In parallel, due to the growing environmental concern, the use of natural fibres in alternative applications motivated further research as they represent a renewable resource and they can be recyclable and biodegradable by the end of their life cycle [Fan 2017], contrary to synthetic fibres, which currently dominate the field of strengthening applications. Owing to their low density and good mechanical properties (with tensile strength, stiffness and deformability appropriate for structural applications), natural fibres are suitable to form structural “green” composites and have the potential to substitute petroleum-based composites [Netravali 2007].

Extensive research has been carried out in the field of cementitious composites reinforced with short dispersed natural fibres (NFRC) and in the field of natural fibre reinforced polymers (NFRP). However, the structural performance of natural fibre fabrics/textiles combined with inorganic matrices (NTRM/NFRCM) as strengthening systems has been the object of only a few studies and their tensile and bond behaviour at a composite level are still little understood. As in the case of more established TRM systems, the properties of NTRM constituents (i.e. yarns, textiles and matrix) cannot be used individually to predict the behaviour of the corresponding composites, due to the complicated stress-transfer mechanism at the fibre/matrix interface [D’Antino 2017].

This paper examines the feasibility of using flax and jute grids embedded in lime-based mortar (forming composites belonging to the family of Textile-

Reinforced Mortar - TRM) as externally bonded strengthening systems for masonry. Flax and jute are natural fibres of vegetable origin that have been reported to have comparable mechanical properties to those of E-glass fibres [e.g. Codispoti 2015] and could be also used in cases where the cost of the latter is prohibitive. In parallel, the use of lime-based mortar does not cause significant degradation of the long-term natural fibre properties [Wei 2015], while it still allows the masonry substrate to "breathe" and provides a sustainable solution. Both constituents, i.e. fibres and mortar, are environmentally friendly, cost-effective and easy to source/make, enabling their application in both developed and developing countries.

2 EXPERIMENTAL PROGRAMME

Three series of direct tensile tests were carried out on different types of fibres, textiles and NTRM composites to fully characterize their mechanical performance. The specimens comprised:

1. bare flax and jute yarns;
2. bare flax and jute textiles;
3. flax- and jute-TRM composites.

2.1 Materials

All textiles (Fig. 1) were balanced bidirectional, with properties as summarised in Tab. 1. The yarn diameter for both flax types was calculated as the ratio of linear/bulk density (given by the supplier), while for jute it was estimated as an average of 50 measurements (10 cross sections on each of 5 different samples) using a Nikon optical microscope (CoV 27%). The yarn cross-sectional area was assumed circular and constant during the tensile tests.

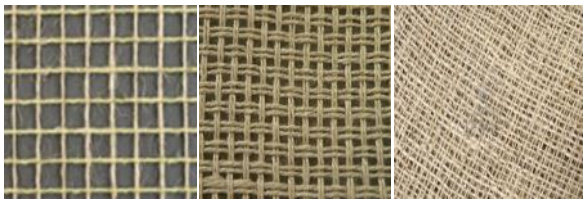

Fig. 40: flax1, flax2 and jute (from left to right).

Tab. 5: Textile properties.

Textile, ID	Mesh size (mm)	Weight* (g/m^2)	Yarn Area (mm^2)
Flax1, F1	14 x 14	215	1.10
Flax2, F2	4 x 4	300	0.22
Jute, J	2 x 2	183	0.25

*taken from data sheets.

The inorganic matrix was a lime-based mortar (NHL 2) containing siliceous and calcareous aggregates with a flexural and compressive strength (at 28 days) of 2.8 MPa and 7.7 MPa, respectively.

2.2 Preparation of NTRM coupons

Eighteen NTRM coupons measuring 600 x 50 x 6 mm were manufactured (Fig. 2), consisting of a single textile layer positioned in the middle of the coupon (3-mm thick bottom and top mortar layer). Specimens were wet-cured for a period of 28 days and then kept in standard laboratory conditions until testing. The face cast against the mould was prepared manually with a random speckle pattern in order to measure the displacement field along the free length of the coupon by Digital Image Correlation (DIC).

(a) (b)

Fig. 41: Preparation of NTRM coupons : (a) Textile embedment in the mortar; (b) application of top mortar layer.

2.3 Experimental Setup

The ends of the yarns were secured on the side of the jaws by means of bolts, leaving a free length of 300 mm. In the case of yarns, a disc placed in the gripping jaws of the machine was used to wrap the yarn twice around it (Fig.3a). To apply the load uniformly, the ends of both textile specimens and coupons were fitted with a pair of aluminum tabs, glued by means of a high-strength epoxy. The textiles were gripped directly in the wedges of the machine resulting in a free length of 200 mm (Fig.3b), while clevis-type grips were implemented for NTRM coupons resulting in a free length of 320 mm (Fig.3c).

All tests were carried out in a universal testing machine under displacement control. Yarns and textiles were tested at 300 mm/min, according to [EN ISO 2062 2009] and at 2 mm/min, following practices in published research studies [e.g. Ghiassi 2015], respectively. NTRM coupons were loaded at 0.2 mm/min until the first crack and 1mm/min thereafter. Due to the texture of the natural fibres and their flexibility as well as the fragility of the coupons, only contactless measurements could be used. Therefore, DIC was employed since its reliability has been proven in several studies [e.g. Tekieli 2017]. In the case of the bare textiles, an optimized computer generated speckle pattern was glued on the tabs and on 4-mm diameter markers. Rows of markers were glued along the longitudinal yarns, one near each clamping region and additional two at the mid-length of the specimen spaced apart approximately 50 mm (Fig. 4). Each row consisted of three markers evenly spaced along the width of the specimen. The strain data were derived from DIC by measuring the displacement near the edges of the gripping tabs. Additional data on the strain of the individual yarns of the bare textile were acquired by tracking the displacement of the 4-mm markers. Similarly, displacement measurements on the NTRM composites were performed by monitoring their free length. A speckled reference target was positioned next to each specimen, in both bare textiles and coupons, to eliminate the influence of any external vibration. Photos were acquired every 1 s and were processed with the *GOM Correlat*e software program [GOM 2017].

(a) (b) (c)

Fig. 42: Clamping details for (a) yarns ; (b) bare textiles and (c) NTRM coupons.

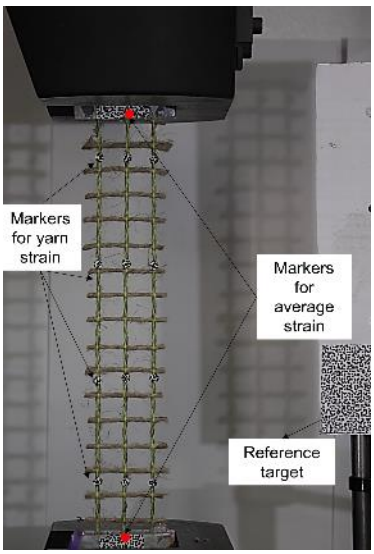

Fig. 43: Typical configuration of markers for DIC analyses (F1 textile).

3 EXPERIMENTAL RESULTS

3.1 Yarns

Twenty yarns from each fibre type were tested in direct tension and the average values of tensile strength $\sigma_{f,y}$, strain at failure $\varepsilon_{f,y}$, and corresponding Young's modulus $E_{f,y}$ are summarised in Tab. 2 (CoV values are given in brackets). All yarns failed due to rupture, which occurred away from the clamps at large deformation. Higher values of tensile strength and stiffness were obtained by both flax types, with yarns extracted from the denser and of smaller diameter mesh (F2) showing better performance. The stress-strain response (Fig. 5) was non-linear at lower loads due to lack of straightness of the individual filaments, and linear up to failure. Larger diameter flax yarns (F1) showed a more progressive failure, possibly due to the non-uniform stress transfer across the yarn cross-section (shear lag effect).

Tab. 6: Natural yarn tensile properties.

Yarn Type	$\sigma_{f,y}$ (MPa)	$\varepsilon_{f,y}$ (%)	$E_{f,y}$ (GPa)
F1	212.6	6.71	5.39
	(0.09)	(0.10)	(0.12)
F2	377.9	9.17	7.61
	(0.07)	(0.05)	(0.07)
J	121.0	6.06	3.43
	(0.17)	(0.12)	(0.10)

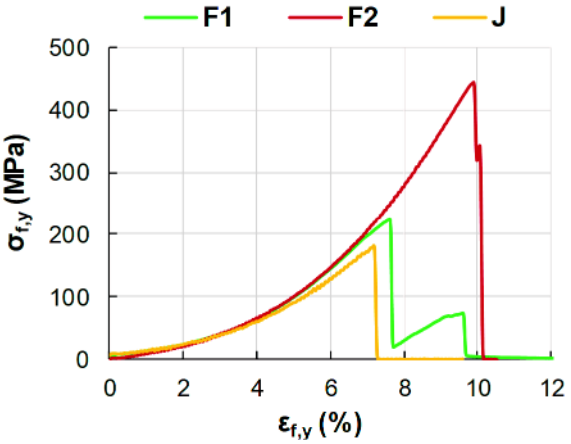

Fig. 44: Typical tensile behaviour of F1, F2 and jute yarns.

3.2 Bare Textiles

Textiles F1 comprised 3 yarns along their width, while textiles F2 and J included 20 yarns, resulting in a textile area of 3.4 mm^2 for F1, 4 mm^2 for F2, and 5 mm^2 for jute. The resulting tensile properties of the tested bare textiles (average values of 5 specimens per fibre type) are reported in Tab. 3, in terms of tensile strength $\sigma_{f,t}$, strain at failure $\varepsilon_{f,t}$ and Young's modulus $E_{f,t}$. Good repeatability of the results was achieved as shown by the low CoV values given in brackets.

Tab. 7: Natural textile tensile properties.

Textile Type	$\sigma_{f,t}$ (MPa)	$\varepsilon_{f,t}$ (%)	$E_{f,t}$ (GPa)
F1	194.3	4.04	6.8
	(0.12)	(0.09)	(0.11)
F2	288.2	3.55	12.8
	(0.07)	(0.03)	(0.17)
J	97.9	1.54	11.1
	(0.16)	(0.10)	(0.06)

The obtained typical stress-strain response curves of the tested textiles are plotted in Fig. 6. The tensile behaviour of all the textiles was similar to that of the corresponding yarns: an initial inelastic branch followed by a linear one up to failure, which occurred progressively. The failure mode was different between the fibre types: In F2 and J textiles, failure was caused by the progressive rupture of the yarns away from the clamps, which was possibly facilitated by the small diameter and the denser mesh. On the contrary, F1 textiles, which are characterised by a significantly larger diameter yarns, failed due to rupture of the individual filaments across the yarns and not of the whole yarns. The presence of the glued markers did not affect the failure mode as rupture in all specimens always occurred away from their location.

Better mechanical performance was achieved by F2 textiles (as also observed from the direct tests on the single yarns), while jute textiles exhibited lower strength but similar stiffness to F2. F1 textiles were characterised by the largest ultimate elongation and the lowest stiffness, similar to that of the corresponding single yarn.

Strains measurements along the individual yarns of the textile, which were obtained by DIC analyses, confirmed that the adopted setup resulted in a uniform stress distribution along the majority of the specimen. An

indicative stress-strain response is given in Fig. 7. The yarns forming the textile failed at a level of stress that was always lower than the maximum strength of the same yarn tested individually.

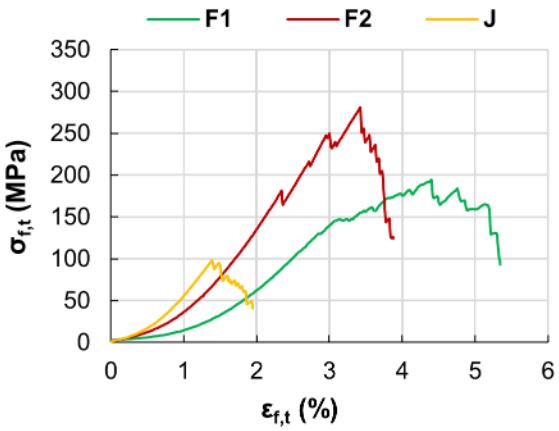

Fig. 45: Typical stress-strain behaviour of textiles made of F1, F2 and jute fibres.

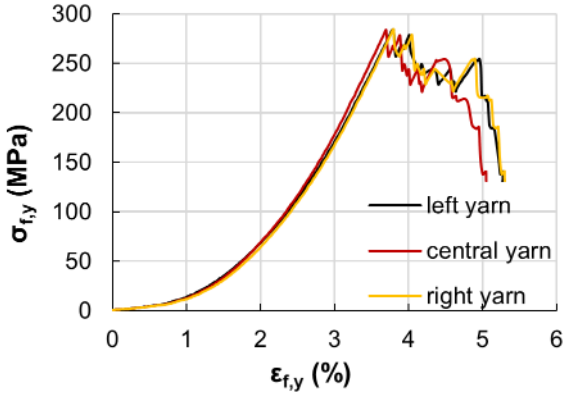

Fig. 46: Typical stress-strain response of individual yarns of the textile specimen (F2).

3.3 NTRM Composites

The results of the tensile tests on the NTRM coupons are summarised in Tab. 4 in terms of average maximum strength σ_{fu}, strain at failure ε_{ffu}, and Young's modulus E_f, at the cracked stage (CoV values are given in brackets). The stress was calculated by dividing the load by the cross-sectional area of the textile, equal to 3.34 mm^2, 4 mm^2 and 2.5 mm^2 for F1, F2 and J, respectively. Specimens were named following the notation NL1-n, where N is the type of the natural fibre used (F1, F2 or J) and n the number of replicate. Fig. 8 shows a representative stress-strain response of different natural-fibre reinforced specimens.

Tab. 8: Natural-fibre TRM tensile properties.

Specimen ID	σ_{fu} (MPa)	ε_{ffu} (%)	E_f (GPa)
F1L1	82	2.25	2.0
	(0.16)	(0.29)	(0.17)
F2L1	192	5.21	4.0
	(0.14)	(0.20)	(0.30)
JL1	31	0.90	4.2
	(0.11)	(0.28)	(0.24)

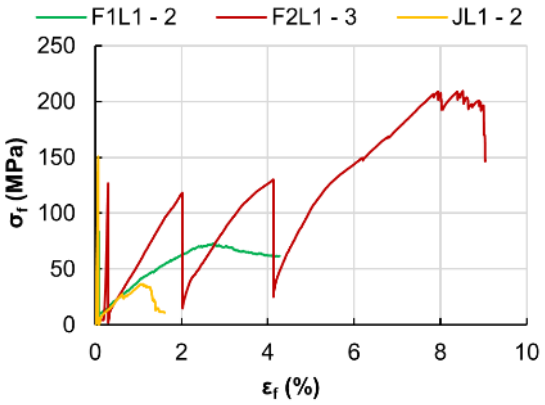

Fig. 47: Typical tensile behaviour of F1-, F2- and jute-reinforced TRM specimens.

The typical tensile response of commercially available TRM systems is characterised by three stages: a) uncracked stage, during which the load is taken only by the matrix, b) crack development stage, shown by successive drops in the stress-strain response and multiple crack formation along the composite, during which the matrix and the reinforcement work together and c) cracked stage, during which the load is carried entirely by the textile reinforcement.

These three stages were present in all F2-TRM specimens, with multiple cracks being formed in the lime-based mortar indicating a good distribution of stresses along the composite and sufficient bond at the textile/mortar interface. On the contrary, no strain hardening was observed in the case of J-TRM coupons, as their tensile behaviour was characterised by a single major crack which widened significantly during the test. The stress-strain response of F1-TRM coupons showed a mixed behaviour: two to three cracks occurred in half of the specimens (possibly initiating from pre-existing microcracks), while for the others the crack development stage was entirely absent.

The uncracked stage for some F1- and J-TRM specimens was not always detectable (i.e. absence of the initial linear response). The large diameter of F1 yarns might have caused increased moisture absorption resulting in the development of microcracks prior to testing. Although special care was taken for the manufacturing of the specimens, additional pre-existing microcracks were formed during curing, handling and setting up of the specimens in the test machine. As a result, the uncracked response could not be estimated.

In terms of mechanical performance, the F2-TRM specimens showed the highest tensile strength and ductility. The lowest tensile strength and deformation capacity were attained by J-TRM coupons (as in the case of both yarns and textiles). Comparing flax-TRM composites (F1 and F2), the larger diameter and sparser mesh flax textile (F1) exhibited almost half the tensile capacity of their F2 counterparts.

Notable differences were observed in the failure mode of the NTRM coupons. F2- and J-TRM specimens failed due to the progressive rupture of the individual filaments which reached their tensile strength during the cracked stage. All F1-TRM specimens failed due to slippage within the mortar matrix (combination of pull out and tensile rupture of the filaments), a failure mode also observed in the case of bare F1 textile specimens. Generally, the failure mode of TRM composites under

uniaxial tension is highly dependent on the adopted setup, with clamping grips causing mainly fibre rupture and clevis grips causing mainly slippage [Arboleda 2016]. In this study, the clevis-type grip configuration caused both fibre rupture and slippage, due to the different bond between the different reinforcement types and architecture (mesh size, yarn diameter) and mortar. Typical failure modes are depicted in Fig. 9.

The tensile behaviour of yarns, bare textiles and NTRM coupons is compared in Fig. 10. Clearly, for the same type of natural fibre, the tensile properties of the textile cannot be simply estimated on the basis of the properties of the single yarn. Moreover, when the textile is embedded in the lime-based mortar, overall strength and stiffness are significantly affected, generally resulting in reduced tensile properties and increased deformability. This observation highlights the complex stress-transfer mechanism at the fibre/matrix interface.

Fig. 48: Typical failure modes of F1-, F2- and J-TRM coupons.

Lastly, the development of cracking along the composite during the cracked stage is summarised in Fig. 11 for representative specimens, along with the associated typical strain fields at failure (100% f_{fu}) and the average crack width, $w_{max,avg}$. DIC enabled to detect the exact location of the cracks, even before they become visible, and the information obtained from these measurements can be used to develop analytical models.

4 SUMMARY

This study presents the preliminary results of direct tensile tests on natural fibres in the form of single yarns and textiles and on natural-fibre reinforced lime-based composites. Based on the discussion above, the following conclusions can be drawn:

- Flax fibre yarns showed high deformability (up to 9%) and strength (up to 380 MPa), making them suitable for structural applications.
- The flax textiles with a denser mesh and smaller diameter yarns developed a better mechanical performance.
- Although the jute textile exhibited the lowest strength, a suitable stiffness can be ensured by using an appropriate textile architecture.
- Yarns tested individually always developed higher strength than the average strength measured on the corresponding textiles.
- Lime-based composites reinforced with the smaller diameter flax yarns showed high ductility. Jute and large diameter flax yarns did not perform as well, due to the inherently lower tensile properties of the fibres in the former case and possibly due to poor impregnation of the fibres in the latter case.
- Good bond was observed at the fibre/matrix interface of F2 specimens as evidenced by the formation of multiple cracks.
- DIC enabled accurate detection of the crack pattern (evolution, location, spacing, number and width of cracks) along the composite, values required for the further development of analytical models.

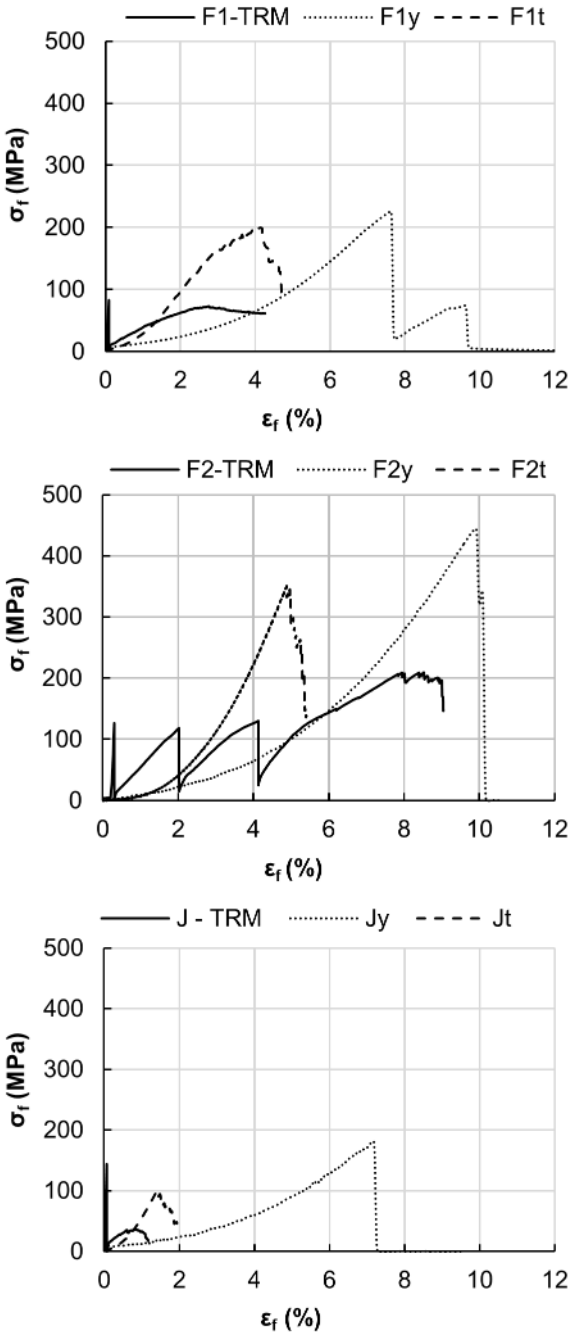

Fig. 49: Typical tensile behaviour of yarn, textile and coupon made of F1, F2 and jute (from top to bottom).

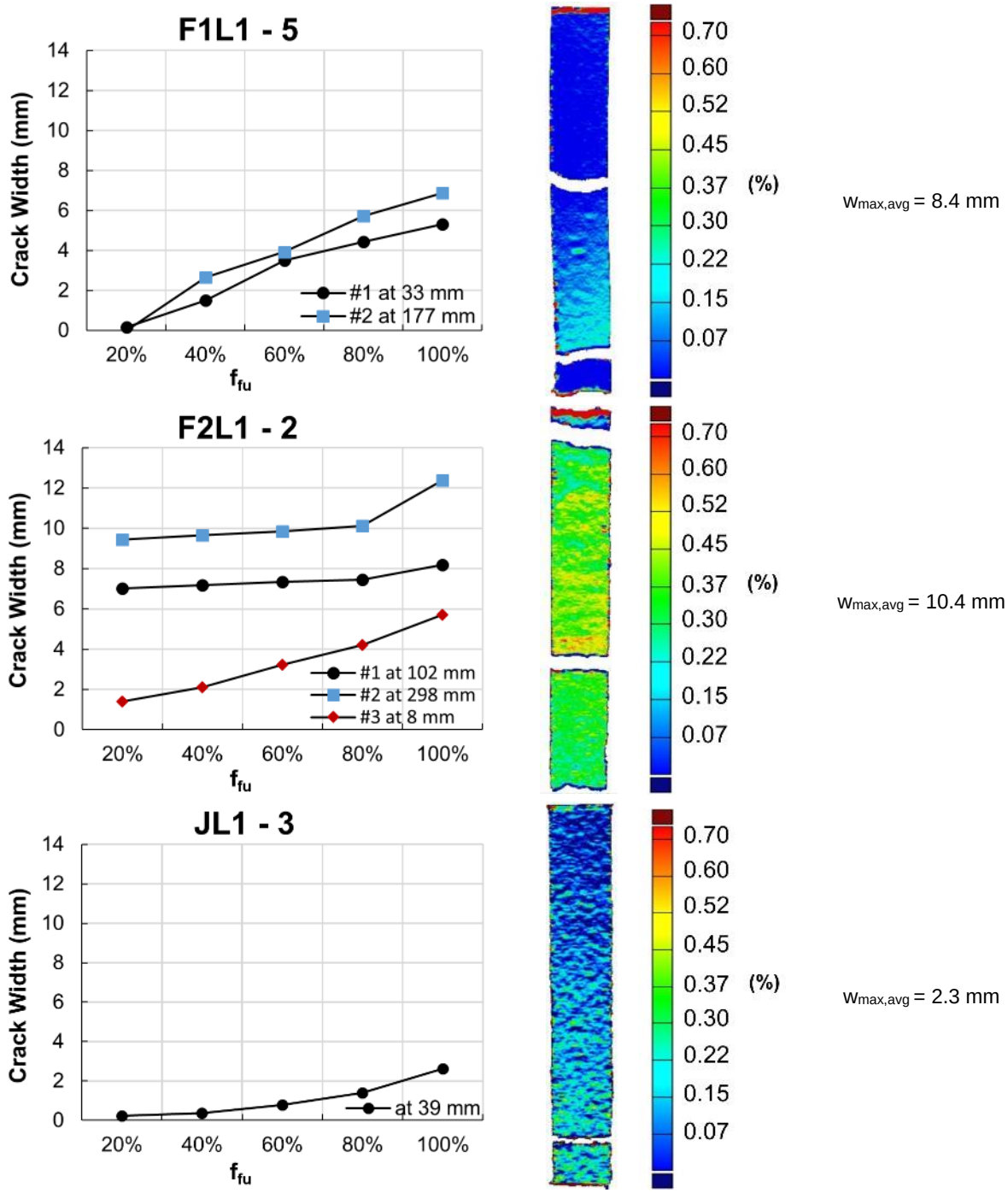

Fig. 50 : Crack development, strain fields at failure and average crack width for representative NTRM coupons.

5 ACKNOWLEDGMENTS

The lime-based mortar and the epoxy adhesive were kindly donated by Vimark S.r.L and Kerakoll S.p.a., respectively. Special thanks to Lisa Barilli and Giorgia Martinelli for the excellent collaboration during the experimental program.

6 REFERENCES

[Arboleda 2016] Arboleda, D.; Carozzi, F. G.; Nanni, A.; Poggi, C.; Testing Procedures for the Uniaxial Tensile Characterization of Fabric-Reinforced Cementitious Matrix Composites. Journal of Composites for Construction, 2016, 20 (3), 1-13.

[Codispoti 2015] Codispoti, R.; Oliveira, D.V.; Olivito, R.S.; Lourenço P. B. et al.; Mechanical performance of natural fiber-reinforced composites for the strengthening of masonry. Composites Part B: Engineering, 2015, 77, 74-83.

[Dittenber 2012] Dittenber D.B.; Gangarao, H.V.S.; Critical review of recent publications on use of natural composites in infrastructure. Composites Part A: Applied Science and Manufacturing, 2012, 43(8), 1419-1429.

[Dunne 2016] Dunne, R.; Desai, D.; Sadiku, R.; Jayaramudu, J.; A review of natural fibres, their sustainability and automotive applications. Journal of Reinforced Plastics and Composites, 2016, 35(13), 1041-1050.

[EN ISO 2062 2009] BSI; Textiles-Yarns from packages-Determination of single-end breaking force and elongation at break using constant rate of extension (CRE) tester.

[Fan 2017] Fan, M.; Future scope and intelligence of natural fibre based construction composites. Duxford: Woodhead Publishing, 2017, 545-556, ISBN: 978-0-08-100411-1.

[Ghiassi 2015] Ghiassi, B., Razavizadeh, A., Oliveira, D.V., Marques, V. et al.; Tensile and bond characterization of natural fibers embedded in inorganic matrices. In: R. Fagueiro, ed. Proceedings of 2nd International Conference on Natural Fibres - From Nature to Market, Azores, Portugal, 27 - 29 April.

[GOM 2017] GOM Correlate Evaluation software for 3D testing [Online]. Available: https://www.gom-corralate.com/en [Accessed 10 January 2017].

[Netravali 2007] Netravali A.N.; Huang, X.; Mizuta, K.; Advanced “green” composites. Advanced Composite Materials: The Official Journal of the Japan Society of Composite Materials, 2007, 16(4), 269-282.

[Wei 2015] Wei, J.; Meyer, C.; Degradation mechanisms of natural fibre in the matrix of cement composites. Cement and Concrete Research, 2015, 73, 1-16.

[Tekieli 2017] Tekieli, M.; De Santis, S.; de Felice, G.; Kwiecien, A. et al.; Application of Digital Image Correlation to composite reinforcements testing. Composites Structures, 2017, 160, 677-688.